

Particle acceleration by strong turbulence in solar flares: theory of spectrum evolution

A.M. Bykov¹,

and

G.D. Fleishman^{2,1}

ABSTRACT

We propose a nonlinear self-consistent model of the turbulent non-resonant particle acceleration in solar flares. We simulate temporal evolution of the spectra of charged particles accelerated by strong long-wavelength MHD turbulence taking into account back reaction of the accelerated particles on the turbulence. The main finding is that the nonlinear coupling of accelerated particles with MHD turbulence results in prominent evolution of the spectra of accelerated particles, which can be either soft-hard-soft or soft-hard-harder depending on the particle injection efficiency. Such evolution patterns are widely observed in hard X-ray and gamma-ray emission from solar flares.

Subject headings: Sun: flares—acceleration of particles—turbulence—diffusion—shock waves—Sun: X-rays, gamma rays

A solar flare arises due to fast and spatially localized strong energy release and reveals itself in electromagnetic radiation and particle flows. Details of the energy release (as well as energy storage) are currently debated. Models based on the idea of magnetic reconnection are the most popular at the moment (Shibata 1999), while interesting alternative possibilities, like ballooning instability (Shibasaki 2001), or circuit models (Zaitsev & Stepanov 1992) are discussed as well.

A common feature of the solar flares (as well as other astrophysical objects with strong energy release) is the production of nonthermal accelerated particles. There are now ample evidence of particle acceleration in flares (Meyer et al. 1956; Mathews & Venkatesan 1990; Cane et al. 1986; Chupp 1990; Akimov et al. 1992). Accelerated electrons reveal themselves

¹Ioffe Institute for Physics and Technology, 194021 St.Petersburg, Russia

²New Jersey Institute of Technology, Newark, NJ 07102

in a variety of nonthermal emissions observed from radio range to gamma-rays. Even rather small number of accelerated electrons arising under a weak acceleration process can be visible when the electrons produce coherent radio emission (e.g., Benz (1986); Fleishman et al. (2002)). Nonthermal incoherent emissions (gyrosynchrotron and/or bremsstrahlung) are detectable when the acceleration is strong enough, providing a considerable fraction of background electrons to be accelerated.

Observations made by Ramaty High Energy Solar Spectroscopic Imager (RHESSI) for the recent years have provided us with new stringent constraints on the acceleration mechanism(s) operating in flares. Grigis & Benz (2004, 2005) investigated spectral evolution during individual subpeaks of the impulsive hard X-ray (HXR) emission and found each such subpeak to display a soft-hard-soft (SHS) evolution; the property, which was earlier established for the impulsive phase as a whole (Parks & Winckler 1969; Kane & Anderson 1970; Benz 1977; Brown & Loran 1985; Lin & Schwartz 1987). Grigis & Benz (2004, 2005) concluded accordingly that the ability to reproduce the SHS spectrum evolution of the accelerated particle population must be an intrinsic property of the acceleration mechanism involved; it is the observational property of the acceleration mechanism that is addressed in this Letter.

A number of acceleration mechanisms and models have been proposed to account for the particle acceleration in flares (see, for a review, Aschwanden (2002)). Acceleration by DC electric fields, both sub-Dreicer and super-Dreicer, has been considered (Holman 1985; Tsuneta 1985; Holman & Benka 1992; Litvinenko 1996). This process is able to provide the energization of particles up to 100 keV, thus, it can be considered as a possible mechanism of pre-acceleration in flares.

Stochastic acceleration by turbulent waves is currently assumed to provide the main acceleration in impulsive solar flares (Miller et al. 1996; Miller 1997; Hamilton & Petrosian 1992; Petrosian et al. 1994; Park et al. 1997; Pryadko & Petrosian 1998), while the classical diffusive shock acceleration is believed to play a role in large-scale gradual events. Miller et al. (1997) made a detailed comparison between various acceleration scenarios and concluded that the stochastic acceleration is intrinsically consistent with the observational constraints on the acceleration time, highest particle energy, and the total number of the accelerated particles. In this Letter we demonstrate that the turbulent stochastic acceleration is also naturally consistent with the SHS spectrum evolution of the accelerated particles.

Grigis & Benz (2006) noticed that within the standard model of the stochastic acceleration (Miller et al. 1996) the higher level of the turbulence results in harder steady-state spectrum of accelerated electrons and vice versa, which looks consistent with the observed SHS evolution. It is, nevertheless, unclear if the real evolution of the spectrum will represent

the sequence of such steady-state spectra or will behave differently. We note, however, that a fraction of stronger events (typically, the proton reach events) displays a different kind of the spectral evolution, namely, soft-hard-harder (SHH) (Frost & Dennis 1971; Cliver et al. 1986; Kiplinger 1995; Saldanha et al. 2008), as well as the gradual phase of the impulsive events (Grigis & Benz 2007); we return to this point later.

Another important point firmly established by RHESSI data analysis (Brown et al. 2007; Dennis et al. 2007; Hudson & Vilmer 2007) is that a significant fraction (some tens of percent) of the released energy goes into nonthermal accelerated particles. This conclusion is also confirmed by the radio data. Bastian et al. (2007) performed a calorimetry of the accelerated electron energy in a solar flare. They analyzed the radio spectrum evolution of a dense flare, when most of the accelerated electron energy was deposited into the coronal loop (rather than into the chromosphere). This made it possible to accurately measure the total energy deposited by the accelerated electrons into the coronal thermal plasma, which turned out to be as high as 30% of the estimated magnetic energy of the flaring loop. These findings imply that the back reaction of the acceleration particles on the accelerating agent (e.g., the turbulence) is not negligible, in full agreement with time-dependent test particle analytical solutions (Bykov & Fleishman 1992) and numerical modeling (Cargill et al. 2006), so this back reaction must be properly taken into account by the acceleration model.

As we have noticed, the stochastic acceleration of the charged particles is the most promising candidate for the particle acceleration in flares (e.g., Miller et al. 1997; Grigis & Benz 2006). However, the mentioned energetic requirements complicate strongly the whole theory of the stochastic acceleration. First of all, the turbulence energy must be large enough to supply the accelerated particles with sufficient energy. This means that the turbulence is strong, so nonlinear effects are important (e.g., Yan et al. 2008) and the (quasilinear) approximation of the weak resonant wave-particle interaction is invalid any longer. Therefore, the theory must include a more general transport equation valid in case of strong large-scale turbulence. Second, since this turbulence loses a large fraction of its energy to accelerate particles, this damping rate must be properly taken into account; thus, one needs to solve two coupled equations – one for the particles and the other for the turbulence.

The renormalized theory of particle acceleration by strong turbulence was developed by Bykov & Toptygin (1990a,b), see the review by Bykov & Toptygin (1993) as well. The form of the equation for the averaged distribution function of nonthermal particles depends on whether the turbulence is composed of smooth (wave-like) fluctuations only or contains also the shock fronts and other discontinuities (Bykov & Toptygin 1993). Observations of the magnetic field complexity in the flare-productive active regions (Abramenko 2005) along with various models of primary energy release in flares (Shibata 1999; Shibasaki 2001;

Zaitsev & Stepanov 1992; Vlahos 2007) suggest many ways of producing long-wave MHD turbulence (e.g., Miller et al. 1997; Grigis & Benz 2006) including possibly a shock wave ensemble (Anastasiadis & Vlahos 1991). Although the generation of discontinuities is likely under the impulsive energy release (e.g., Vlahos 2007), we limit our consideration to the case of smooth long-wave turbulence only, but will include effect of the shocks in a further study.

We, therefore, adopt the following scenario. The process of flare energy release is accompanied by formation of large scale flows and broad spectra of MHD fluctuations in a reasonably tenuous plasma with frozen-in magnetic fields. Vortex electric fields generated by the compressible component of the large scale motions of highly conductive plasma will result in efficient *non-resonant* acceleration of charged particles.

The distribution function $N(\mathbf{r}, p, t)$ of nonthermal particles averaged over an ensemble of turbulent motions satisfies the kinetic equation

$$\frac{\partial N}{\partial t} - \frac{\partial}{\partial r_\alpha} \chi_{\alpha\beta} \frac{\partial N}{\partial r_\beta} = \frac{1}{p^2} \frac{\partial}{\partial p} p^4 D(t) \frac{\partial N}{\partial p} + F_i(p), \quad (1)$$

The particle source term $F_i(p)$ is determined by injection of the electrons and nuclei. Although we do not consider explicitly the injection process, we note that there are many ways to inject particles into the stochastic acceleration by strong turbulence. The possibilities are various versions of the DC acceleration (Litvinenko 1996, 2000, 2003) or resonant stochastic acceleration by the small-scale waves (Miller et al. 1997). A nice option proposed recently by Fletcher & Hudson (2008) is that the reconfiguration of the preflare magnetic field can result in large-scale pulses of the Alfvén waves, which in the presence of strong spatial gradients will generate field-aligned electric regions capable of accelerating electrons from the thermal pool up to 10 keV or above. Our further analysis does not depend on the specific injection mechanism and details of the particle injection process. Then, the phase space diffusion coefficients D and $\chi_{\alpha\beta} = \chi \delta_{\alpha\beta}$ are expressed in terms of the spectral functions that describe correlations between large scale turbulent motions (see Bykov & Toptygin, 1993). The kinetic coefficients satisfy the following renormalization equations:

$$\chi = \kappa + \frac{5}{2} \int \frac{d^3\mathbf{k} d\omega}{(2\pi)^4} \left[\frac{2T + S}{i\omega + k^2\chi} - \frac{2k^2\chi S}{(i\omega + k^2\chi)^2} \right], \quad (2)$$

$$D = \frac{\chi}{9} \int \frac{d^3\mathbf{k} d\omega}{(2\pi)^4} \frac{k^4 S(k, \omega, t)}{\omega^2 + k^4\chi^2}, \quad (3)$$

where $T(k, \omega, t)$ and $S(k, \omega, t)$ are the transverse and longitudinal parts of the Fourier components of the turbulent velocity correlation tensor. The equations for $T(k, \omega, t)$ and $S(k, \omega, t)$

can be found in Bykov (2001). We reproduce here only the equation for the longitudinal spectral function $S(k, \omega, t)$ responsible for the particle acceleration:

$$\frac{\partial S(k, \omega, t)}{\partial t} - \frac{\partial \Pi_\alpha^S(k, \omega, t)}{\partial k_\alpha} = \gamma_{ST}T(k, \omega, t) - \gamma_{dS}S(k, \omega, t) - \gamma_{ap}S(k, \omega, t). \quad (4)$$

This full equation includes nonlinear cascading flux, $\Pi_\alpha^S(k, \omega, t)$, as well as coupling with the transverse function (term $\gamma_{ST}T(k, \omega, t)$), the true damping (term $-\gamma_{dS}S(k, \omega, t)$), and the damping due to acceleration of the charged particles (term $-\gamma_{ap}S(k, \omega, t)$). Although all corresponding processes are generally relevant for the turbulence evolution, we found that only the last of them is critically important to provide the SHS spectrum evolution due to the nonlinear nonresonant particle acceleration by strong turbulence. In case of a single scale long-wavelength injection of the turbulent motions (gaussian spectrum with the characteristic wave-number k_0) we can neglect both cascading term in the left hand side and direct turbulence damping $\gamma_{dS} = 0$. The turbulence is assumed to be confined in the acceleration region; possible turbulence leakage from the acceleration region is compensated by the adopted sustained source of the transverse component of the large-scale turbulence. Particles, however, can escape from the region through its boundaries because of a large mean free path of the particles outside the region. We, therefore, consider a simplified equation for $S(k, \omega, t)$

$$\frac{\partial S(k, \omega, t)}{\partial t} = \gamma_{ST}T(k, \omega, t) - \gamma_{ap}S(k, \omega, t), \quad (5)$$

where the expression for the damping rate of large scale turbulence due to particle acceleration $\gamma_{ap} = \theta D$. The parameter θ was determined (iteratively) in such a way to preserve conservation of the total energy in the system of the turbulence and the particles with account for energetic particle escape from the acceleration region. The standard Crank-Nikolson scheme providing second order accuracy in time evolution was applied to integrate Eqns. (1)–(5). The spatial transport term in Eq. (1) was approximated as (time depending) escape time N/T_{esc} , where $T_{esc} = R^2/4\chi$, R is the characteristic size of the acceleration region. Actually, the temporal evolution of χ is very slow since in Eq. (2) it is dominated by the transverse component of the turbulence $T(k, \omega, t)$, which decays slower than the longitudinal component $S(k, \omega, t)$.

The temporal evolution of the turbulence is, thus, solely due to particle acceleration effect. Particle acceleration time in the model is longer than turn-over time of large scale MHD motions providing $\omega > D$. Our simplified model assumes, therefore, that the turbulence is primary produced in the form of transverse motions with the scale about $2\pi/k_0$ with a gaussian spectrum, which produces the corresponding longitudinal turbulence due to the

mode coupling (term $\gamma_{ST}T(k, \omega, t)$) in a system of a finite scale size R (where $Rk_0 > 1$). Furthermore the model accounts only for the evolution of large scale (energy containing) motions of $k\lambda(p) \ll 1$, where $\lambda(p)$ is particle mean free path due to scattering by small scale (resonant and non-resonant) magnetic field fluctuations; the corresponding diffusion coefficient is $\kappa = v\lambda(p)/3$. We did not consider here the turbulence cascade to resonant (small) scales (c.f. Miller et al. 1996; Petrosian & Bykov 2008). Instead, we fixed the "microscopic" diffusion coefficient $\kappa(p)$ due to small scale fluctuations, provided perhaps by the whistler waves, and considered the case of intensive large scale turbulent motions provided $\kappa(p) < k_0^{-1} \cdot \sqrt{\langle u^2 \rangle}$. The kinetics of particles satisfying this inequality is determined by turbulent advection and so does not depend on the details of the "microscopic" diffusion coefficient.

The energy range, where this inequality holds, does depend on the charged particle mean free path $\lambda(p)$, which is ultimately defined by generally unknown level of the small-scale turbulence. Bastian et al. (2007) determined the mean free path of the radio emitting electrons (a few MeV) to be about 10^7 cm from the characteristic decay time of the radio light curves for the case, when the turbulent transport of the particles was independently confirmed. This estimate is consistent with the small-scale (tens of cm) turbulence level of about $\sim 10^{-7} - 10^{-5}$ derived from the decimetric continuum burst analysis (Nita et al. 2005). Thus, to be conservative, in the case of electrons our approximation is firmly justified at least up to the energy about 1 MeV, where the particle transport is fully driven by the large-scale turbulence and as so it does not depend on the actual momentum dependence of the mean free path $\lambda(p)$. Then the model accounts for a nonlinear backreaction of accelerated particles on large scale motions only. Although the assumed presence of the small-scale turbulence implies the possibility of the stochastic resonant acceleration along with considered here non-resonant acceleration, we do not take into account the resonant acceleration explicitly, because the energy density of the small-scale turbulence is much smaller than that of large-scale turbulence. As has been discussed, the resonant acceleration can, nevertheless, contribute to the injection term $F_i(p)$ in Eq. (1).

We consider injection of non-relativistic particles of a momentum p_0 , i.e. $F_i(p) \propto \delta(p - p_0)$. It is convenient to characterize the injection efficiency by the injection energy loading parameter

$$\zeta_i = \frac{2 \int \epsilon(p) F_i(p) p^2 dp}{D(0) \rho \langle u^2 \rangle}, \quad (6)$$

where $\epsilon(p)$ is the particle kinetic energy expressed via its momentum p . In Figure 1 we show the particle distribution function (normalized $\propto p^2 N$) calculated for the model. We assumed continuous injection of mono energetic particles (electrons and protons $i = e, p$) with the injection energy loading parameters $\zeta_e = 10^{-3}$ (left panel) and $\zeta_e = 0.1$ (right

panel).

Although there are apparent differences in particle spectra for different ζ_e , all our runs display clearly soft-hard-soft behavior of the spectra of accelerated particles. The origin of this spectral evolution is easy to understand within the proposed model. Initial phase of the acceleration occurs in the linear regime (test-particle approximation is still valid on this stage), which results in effective particle acceleration by the longitudinal large scale turbulent motions and spectral hardening. However, fast particles accumulate a considerable fraction of the turbulent energy on this stage and start to exhaust the turbulence, thus, the efficiency of the acceleration decreases, which first affects higher energy particles resulting in the spectrum softening.

Another important point, which must be noticed from the figure, is that the slope of the spectrum at the late decay phase (red solid curves) depends strongly on the injection efficiency ζ_e . In fact, the spectrum is much steeper in case of strong injection. In practice, the spectrum in the right panel is so steep that it is probably undistinguishable against background thermal particle distribution. This means that the sequence of the (dash-dotted) spectra of accelerated electrons in the right panel will reveal itself as SHH evolution of the HXR spectrum. This conclusion is consistent with the fact that the SHH evolution is observed in stronger events, where enhanced injection of the charged particles (e.g., protons) is likely, and with a recent finding of gradual transitions between SHS and SHH evolution fragments (Grigis & Benz 2007), which requires a common acceleration mechanism for both SHS and SHH evolution patterns, even though additional spectral hardening in the gamma-ray range can occur due to relativistic particle trapping in the coronal loops (Krucker et al. 2008).

Besides the general SHS evolution, we should note that in agreement with previous studies of the stochastic acceleration (Miller et al. 1997; Grigis & Benz 2006) the spectra do not obey power-laws exactly: break-up and break-down turning points are evident from the plots. It should be noted here that since the nonlinear effects were taken into account in the model the distribution function calculated for mono-energetic injection will not have any of the general properties of the Green function of a linear system. Therefore, one can not build the distribution function in the nonlinear case using the superposition principle any longer. Nevertheless, the initial stage of the particle acceleration occurs in the linear regime if the loading parameter ζ_e is smaller than unity. Thus, broadly speaking, the general behavior of particle spectra evolution as it is illustrated in Figure 1 will hold for other relatively narrow (as the first blue curves in Figure 1) initial particle distributions with a similar loading parameter defined by Eq. (6).

Grigis & Benz (2006) demonstrated that the HXR spectra from the thin-target coro-

nal sources are the most directly linked to the energy spectra of the accelerated electrons, while the properties of the thick-target foot-point sources can essentially be affected by the transport effects. Accordingly, we computed the evolution of the thin-target HXR emission generated by the evolving ensemble of the accelerated electrons (as in Fig. 1) and then derived the evolution of the HXR spectral index at $E = 35$ keV to compare with the observations of the coronal HXR sources reported by Battaglia & Benz (2006). The theoretical dependences of the HXR spectral index on time are shown in Figure 2 by three curves with different ratio of the acceleration time to the escape time. The asterisks in the same plot show the evolution of the HXR spectral index observed for the coronal source in the Dec., 04, 2002 event (Battaglia & Benz 2006). Even though no theoretical curve is the exact fit to the data, one can clearly note important similarities between theoretical and observational curves including the main SHS behavior and some hardening at the later stage.

Since the spectral index analysis of the coronal source can in principle be biased by much stronger foot-point contribution, a more reliable way of the thin-target HXR analysis could be the study of the occulted X-ray flares. However, the thin-target HXR flux is typically weak from the occulted coronal sources, so the systematic statistical study of the occulted flares reports only the spectral data at around the peak time of the flare (Krucker & Lin 2008). In some cases, however, it is still possible to derive information on the spectral evolution of the occulted flares by integrating the signal during rise, peak, and decay phases respectively. An example of the corresponding spectral index evolution in an occulted 06 Sept. 2002 flare is shown by three long horizontal dashes in Figure 2 (E. Kontar, private communication). The SHS evolution is evident in this instance as well.

In addition to the mentioned similarities between the theoretical and the observed spectra, there are also apparent differences. We have to note, however, that the differences between the theory and observations are less significant than the difference between the spectra observed from different events. Thus, we can ascribe these differences to the varying geometry of the source and/or to different regimes of the turbulence generation, cascading, damping, and escape, i.e., to those details of the model, which have not been specifically addressed within this letter.

To summarize, we note that taking into account the nonlinearity, which is necessarily present in a system where efficient acceleration by strong turbulence occurs, offers a plausible way of interpreting both kinds of the characteristic spectrum evolution, SHS and SHH, observed from solar flares. A side achievement of the adopted here model of the turbulent electron transport is the energy independent escape time from the acceleration region, which implies that electrons with different energies leave the acceleration site simultaneously: the property required by measurements of the HXR fine structure timing (Aschwanden 2002). A

full comprehensive picture of the particle acceleration in flares will require further analysis with the shock waves, turbulence cascading, and injection details included, as well as computing the HXR and gamma-ray spectrum evolution, which we plan to consider elsewhere.

We are cordially grateful to Marina Battaglia for providing us with the data on the spectral index evolution from the coronal sources, and to Eduard Kontar, who obtained and provided us with the data on the spectral evolution of the occulted 06 Sept. 2002 flare. The work was partly supported by Russian Foundation for Basic Research, grants No.06-02-16844, 06-02-16295, 08-02-92228, 09-02-00624 and by NSF grants AST-0607544 and ATM-0707319 to New Jersey Institute of Technology. We have made use of NASA's Astrophysics Data System Abstract Service.

REFERENCES

- Abramenko, V. I. 2005, *ApJ*, 629, 1141
- Akimov, V. V., Afanasev, V. G., Belousov, A. S. et al. 1992, *Sov. Astron. Lett.*, 18, 69
- Anastasiadis, A. & Vlahos, L. 1991, *A&A*, 245, 271
- Aschwanden, M. J. 2002, *Particle Acceleration and Kinematics in Solar Flares (Particle Acceleration and Kinematics in Solar Flares, A Synthesis of Recent Observations and Theoretical Concepts, by Markus J. Aschwanden, Lockheed Martin, Advanced technology Center, palo Alto, California, U.S.A. Reprinted from SPACE SCIENCE REVIEWS, Volume 101, Nos. 1-2 Kluwer Academic Publishers, Dordrecht)*
- Bastian, T. S., Fleishman, G. D., & Gary, D. E. 2007, *ApJ*, 666, 1256
- Battaglia, M. & Benz, A. O. 2006, *A&A*, 456, 751
- Benz, A. O. 1977, *ApJ*, 211, 270
- . 1986, *Sol. Phys.*, 104, 99
- Brown, J. C., Kontar, E. P., & Veronig, A. M. 2007, in *Lecture Notes in Physics*, Berlin Springer Verlag, Vol. 725, *Lecture Notes in Physics*, Berlin Springer Verlag, ed. K.-L. Klein & A. L. MacKinnon, 65–+
- Brown, J. C. & Loran, J. M. 1985, *MNRAS*, 212, 245
- Bykov, A. M. 2001, *Space Science Reviews*, 99, 317

- Bykov, A. M. & Fleishman, G. D. 1992, MNRAS, 255, 269
- Bykov, A. M. & Toptygin, I. N. 1990a, Zhurnal Eksperimental noi i Teoreticheskoi Fiziki, 97, 194
- . 1990b, Zhurnal Eksperimental noi i Teoreticheskoi Fiziki, 98, 1255
- . 1993, Physics – Uspekhi, 36, 10201052
- Cane, H. V., McGuire, R. E., & von Rosenvinge, T. T. 1986, ApJ, 301, 448
- Cargill, P. J., Vlahos, L., Turkmani, R., Galsgaard, K., & Isliker, H. 2006, Space Science Reviews, 124, 249
- Chupp, E. L. 1990, ApJS, 73, 213
- Cliver, E. W., Dennis, B. R., Kiplinger, A. L., Kane, S. R., Neidig, D. F., Sheeley, Jr., N. R., & Koomen, M. J. 1986, ApJ, 305, 920
- Dennis, B. R., Hudson, H. S., & Krucker, S. 2007, in Lecture Notes in Physics, Berlin Springer Verlag, Vol. 725, Lecture Notes in Physics, Berlin Springer Verlag, ed. K.-L. Klein & A. L. MacKinnon, 33–+
- Fleishman, G. D., Fu, Q. J., Wang, M., Huang, G.-L., & Melnikov, V. F. 2002, Phys. Rev. Lett., 88, 251101
- Fletcher, L. & Hudson, H. S. 2008, ApJ, 675, 1645
- Frost, K. J. & Dennis, B. R. 1971, ApJ, 165, 655
- Grigis, P. C. & Benz, A. O. 2004, A&A, 426, 1093
- . 2005, A&A, 434, 1173
- . 2006, A&A, 458, 641
- . 2007, ArXiv e-prints, 708
- Hamilton, R. J. & Petrosian, V. 1992, ApJ, 398, 350
- Holman, G. D. 1985, ApJ, 293, 584
- Holman, G. D. & Benka, S. G. 1992, ApJ, 400, L79

- Hudson, H. & Vilmer, N. 2007, in *Lecture Notes in Physics*, Berlin Springer Verlag, Vol. 725, *Lecture Notes in Physics*, Berlin Springer Verlag, ed. K.-L. Klein & A. L. MacKinnon, 81–+
- Kane, S. R. & Anderson, K. A. 1970, *ApJ*, 162, 1003
- Kiplinger, A. L. 1995, *ApJ*, 453, 973
- Krucker, S., Hurford, G. J., MacKinnon, A. L., Shih, A. Y., & Lin, R. P. 2008, *ApJ*, 678, L63
- Krucker, S. & Lin, R. P. 2008, *ApJ*, 673, 1181
- Lin, R. P. & Schwartz, R. A. 1987, *ApJ*, 312, 462
- Litvinenko, Y. E. 1996, *ApJ*, 462, 997
- . 2000, *Sol. Phys.*, 194, 327
- . 2003, *Advances in Space Research*, 32, 2385
- Mathews, T. & Venkatesan, D. 1990, *Nature*, 345, 600
- Meyer, P., Parker, E. N., & Simpson, J. A. 1956, *Physical Review*, 104, 768
- Miller, J. A. 1997, *ApJ*, 491, 939
- Miller, J. A., Cargill, P. J., Emslie, A. G., Holman, G. D., Dennis, B. R., LaRosa, T. N., Winglee, R. M., Benka, S. G., & Tsuneta, S. 1997, *J. Geophys. Res.*, 102, 14631
- Miller, J. A., Larosa, T. N., & Moore, R. L. 1996, *ApJ*, 461, 445
- Nita, G. M., Gary, D. E., & Fleishman, G. D. 2005, *ApJ*, 629, L65
- Park, B. T., Petrosian, V., & Schwartz, R. A. 1997, *ApJ*, 489, 358
- Parks, G. K. & Winckler, J. R. 1969, *ApJ*, 155, L117+
- Petrosian, V. & Bykov, A. M. 2008, *Space Science Reviews*, 134, 207
- Petrosian, V., McTiernan, J. M., & Marschhauser, H. 1994, *ApJ*, 434, 747
- Pryadko, J. M. & Petrosian, V. 1998, *ApJ*, 495, 377
- Saldanha, R., Krucker, S., & Lin, R. P. 2008, *ApJ*, 673, 1169

Shibasaki, K. 2001, *ApJ*, 557, 326

Shibata, K. 1999, *Ap&SS*, 264, 129

Tsuneta, S. 1985, *ApJ*, 290, 353

Vlahos, L. 2007, in *Lecture Notes in Physics*, Berlin Springer Verlag, Vol. 725, *Lecture Notes in Physics*, Berlin Springer Verlag, ed. K.-L. Klein & A. L. MacKinnon, 15–+

Yan, H., Lazarian, A., & Petrosian, V. 2008, *ArXiv e-prints*, 801

Zaitsev, V. V. & Stepanov, A. V. 1992, *Sol. Phys.*, 139, 343

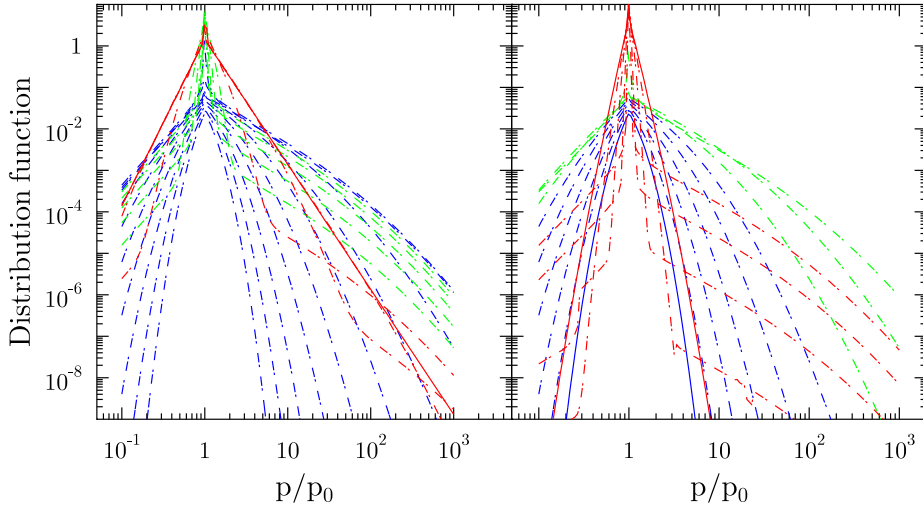


Fig. 1.— The temporal evolution of particle distribution function (sequence of $p^2 N$ vs p/p_0 plots, where p/p_0 is the dimensionless particle momentum normalized by the injection momentum p_0) simulated within a flare acceleration region of the scale size $R = 14\pi/k_0$ for the particle injection energy loading parameters $\zeta_i = 10^{-3}$ (left panel) and $\zeta_i = 0.1$ (right panel). Particle spectra are shown in 20 logarithmically distributed consequent time frames measured in $t D(0)$ starting from 0.01 to 30. For some typical parameters, e.g., $R = 2 \times 10^9$ cm, $B=300$ G, $n = 10^9 - 10^{11}$ cm $^{-3}$ we have $v_A \simeq 2.2 \times (10^8 - 10^9)$ cm/s, and the characteristic acceleration time $\tau_{acc} \equiv 1/D(0) \simeq 1-10$ s in agreement with HXR (Grigis & Benz 2006) and radio (Bastian et al. 2007) observations.

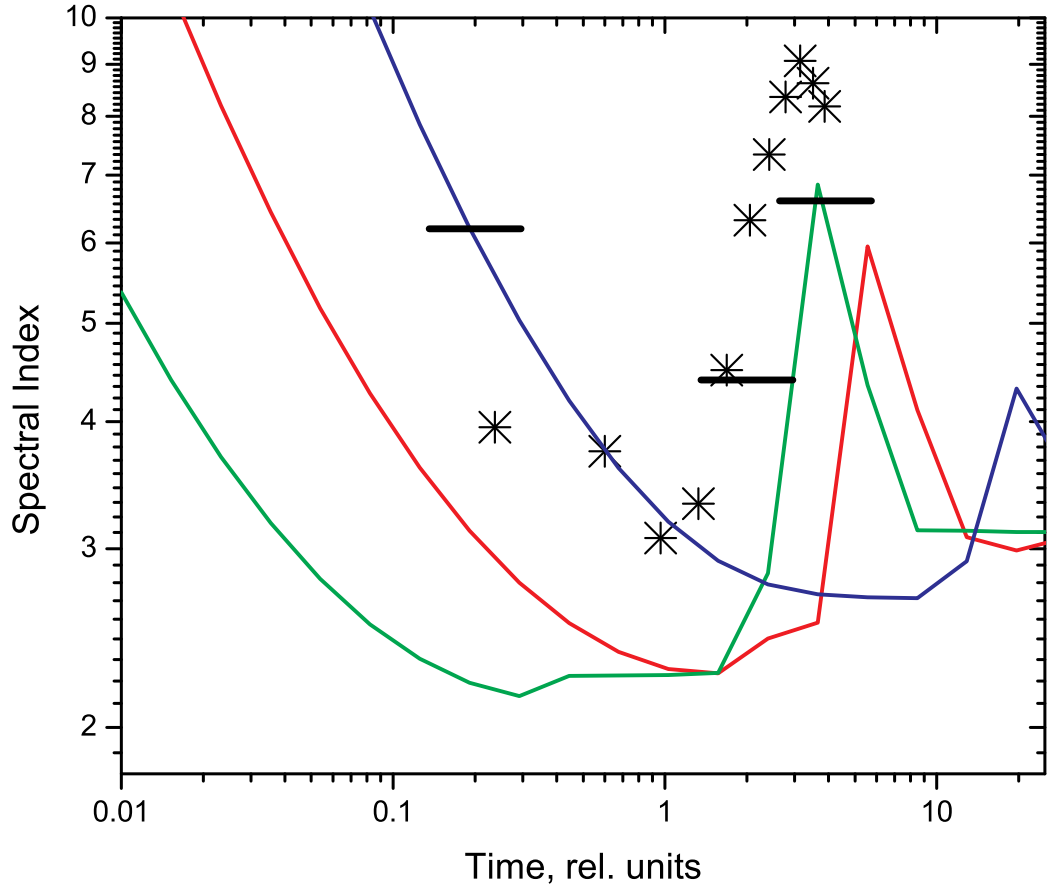


Fig. 2.— HXR spectral index evolution for theoretically calculated spectra with various ratios of the escape time to the acceleration time, $T_{esc}/\tau_{acc} = 5$ (solid curve), 1 (dashed curve), and 0.2 (dash-dotted curve); and observed from the 04 Dec. 2002 flare, asterisks, (Battaglia & Benz 2006), and from the occulted 06 Sept. 2002 flare, horizontal dashes, (E.Kontar, private communication) .